

Quantum nature of proton transferring across one-dimensional potential fields

Cheng Bi(毕成), Quan Chen (陈泉), Wei Li(李伟), and Yong Yang(杨勇)

Citation: Chin. Phys. B, 2021, 30 (**4**): 046601. DOI: 10.1088/1674-1056/abe114
Journal homepage: http://cpb.iphy.ac.cn; http://iopscience.iop.org/cpb

What follows is a list of articles you may be interested in

Charge trapping memory device based on the Ga_2O_3 films as trapping and blocking layer

Bing Bai(白冰), Hong Wang(王宏), Yan Li(李岩), Yunxia Hao(郝云霞), Bo Zhang(张博), Boping Wang(王博平), Zihang Wang(王子航), Hongqi Yang(杨红旗), Qihang Gao(高启航), Chao Lü(吕超), Qingshun Zhang(张庆顺), Xiaobing Yan(闫小兵)

Chin. Phys. B, 2019, 28 (**10**): 106802. DOI: 10.1088/1674-1056/ab3e62

Co-adsorption of O_2 and H_2O on α-uranium (110) surface: A density functional theory study

Xin Qu(瞿鑫), Ru-Song Li(李如松), Bin He(何彬), Fei Wang(王飞), Kai-Long Yuan(袁凯龙)

Chin. Phys. B, 2018, 27 (**7**): 076501. DOI: 10.1088/1674-1056/27/7/076501

Effect of deposited temperatures of the buffer layer on the band offset of CZTS/In_2S_3 heterostructure and its solar cell performance

Jinling Yu(俞金玲), Zhongming Zheng(郑重明), Limei Dong(董丽美), Shuying Cheng(程树英), Yunfeng Lai(赖云锋), Qiao Zheng(郑巧), Haifang Zhou(周海芳), Hongjie Jia(贾宏杰), Hong Zhang(张红)

Chin. Phys. B, 2017, 26 (**4**): 046802. DOI: 10.1088/1674-1056/26/4/046802

Skin formation in drying a film of soft matter solutions: Application of solute based Lagrangian scheme

Ling Luo(罗凌), Fanlong Meng(孟凡龙), Junying Zhang(张俊英), Masao Doi

Chin. Phys. B, 2016, 25 (**7**): 076801. DOI: 10.1088/1674-1056/25/7/076801

Adsorption behavior of Fe atoms on a naphthalocyanine monolayer on Ag(111) surface

Yan Ling-Hao, Wu Rong-Ting, Bao De-Liang, Ren Jun-Hai, Zhang Yan-Fang, Zhang Hai-Gang, Huang Li, Wang Ye-Liang, Du Shi-Xuan, Huan Qing, Gao Hong-Jun

Chin. Phys. B, 2015, 24 (**7**): 076802. DOI: 10.1088/1674-1056/24/7/076802

Quantum nature of proton transferring across one-dimensional potential fields*

Cheng Bi(毕成)[1,2], Quan Chen (陈泉)[1], Wei Li(李伟)[3], and Yong Yang(杨勇)[1,2,†]

[1] *Key Laboratory of Photovoltaic and Energy Conservation Materials, Institute of Solid State Physics, HFIPS, Chinese Academy of Sciences, Hefei* 230031, *China*

[2] *Science Island Branch of Graduate School, University of Science and Technology of China, Hefei* 230026, *China*

[3] *Key Laboratory of Materials Physics, Institute of Solid State Physics, HFIPS, Chinese Academy of Sciences, Hefei* 230031, *China*

(Received 21 December 2020; revised manuscript received 21 January 2021; accepted manuscript online 29 January 2021)

Proton transfer plays a key role in the applications of advanced energy materials as well as in the functionalities of biological systems. In this work, based on the transfer matrix method, we study the quantum effects of proton transfer in a series of one-dimensional (1D) model potentials and numerically calculate the quantum probability of transferring across single and double barriers (wells). In the case of single barriers, when the incident energies of protons are above the barrier height, the quantum oscillations in the transmission coefficients depend on the geometric shape of the barriers. It is found that atomic resonant tunneling (ART) not only presents in the rectangular single well and rectangular double barriers as expected, but also exists in the other types of potential wells and double barriers. For hetero-structured double barriers, there is no resonant tunneling in the classical forbidden zone, i.e., in the case when the incident energy (E_i) is lower than the barrier height (E_b). Furthermore, we have provided generalized analysis on the characteristics of transmission coefficients of hetero-structured rectangular double barriers.

Keywords: proton transfer, nuclear quantum effects, atomic resonant tunneling, double barriers

PACS: 66.30.jp, 68.35.Fx, 82.40.–g **DOI:** 10.1088/1674-1056/abe114

1. Introduction

Proton transfer plays an important role in many fields of physics, chemistry, and biological systems. A typical system is the mixed atomic and molecular phase of solid hydrogen and deuterium.[1] Based on *in-situ* optical spectroscopy measurements, Howie *et al.* have investigated the spectral features of the phase IV–III transition and shown that the large differences in the peak widths of the isotopes Raman spectra indicate the presence of proton tunneling in phase IV.[1] *Ab initio* variable-cell molecular dynamics (MD) simulations have been carried out to study the dynamical properties of phase IV of solid hydrogen and deuterium at high pressures and a temperature range of 300–500 K,[2] aiming to identify the intralayer proton or deuteron transfer and the simultaneous rotation of three-molecule rings in layer II of phase IV. It is found that proton transfer has a direct relation to the unique elongation of molecules in layer II, as well as the lifetime and anharmonic vibrations of the hydrogen molecules.[2]

In biochemistry, the mechanism of proton transfer reveals the light-driven process of biological chromophores. Excited state intramolecular proton transfer is a photochemical process that produces a tautomer with a different electronic structure from the original excited form.[3–8] Using state-of-the-art experimental techniques, such as time-resolved photoelectron imaging measurements, it is possible to see how the addition of a single hydrogen bond and the opening of an excited state proton transfer channel would change the product of a photochemical reaction, and to explore the mechanism of excited state proton transfer process within a single hydrogen bond in simple systems like ammonia dimer.[9]

The proton transfer process in the aqueous-phase reactions has also attracted attention. In a recent study which uses *ab initio* molecular dynamics to simulate the diffusion of protons between the Brønsted acid site (BAS) and the water molecules in the zeolite pores, it is shown that water clusters of different sizes will greatly affect the competition of proton hopping between the O atoms of BAS sites and within the water clusters.[10] In addition, proton transfer in liquid water is intimately connected to the reorganization of the hydrogen-bonded network of the water solvent. Sofronov and Bakker reported that nanoconfinement leads to very strong slow-down effects on the rate of aqueous proton transfer.[11]

With the recent development of machine learning, new theoretical approaches such as neural networks have been introduced to explore the process of proton transfer. Based on the combination of the computationally efficient neural network potential with enhanced sampling techniques, Andrade *et al.* have constructed the free energy surface for water and proton transport at the TiO_2–liquid water interface and performed MD simulations to study the dynamics of interfacial water at time scales well beyond traditional *ab initio* MD.[12] Their simulation results support a picture of predom-

*Project supported by the National Natural Science Foundation of China (Grant No. 11474285).

†Corresponding author. E-mail: yyanglab@issp.ac.cn

© 2021 Chinese Physical Society and IOP Publishing Ltd

inantly molecular adsorption on the defect-free anatase TiO_2 (101) surface in contact with liquid water at ambient conditions, with a tiny fraction ($\sim 5.6\%$) of water dissociation at the interface.[12] This work not only solves the longstanding problem of whether or not water would dissociate spontaneously on defect-free anatase TiO_2 (101), but also demonstrates the vital role of proton transfer in the adsorption form of interfacial water.

In the process of proton transport, the nuclear quantum effects (NQEs),[13–16] that is, the quantum motion of hydrogen atoms, play an important role. Accurate measurement and analysis of the nuclear quantum effects of hydrogen atoms are challenging both theoretically and experimentally. Recent progress in experimental techniques of measurements includes deep inelastic neutron scattering[17,18] and inelastic electron tunneling spectroscopy.[19] For precise theoretical research, path integral molecular dynamics (PIMD) using interaction potentials from first-principles, i.e., *ab initio* PIMD,[20] is mainly employed. Due to the huge amounts of computational resources required in *ab initio* PIMD calculations, it is extremely difficult to apply this method to deal with the NQEs of hydrogen atoms during their transport processes. Apparently, alternative approaches are prerequisites to treat the NQEs of proton transfer.

Recently, based on the method of transfer matrix (TM) in combination with first-principles calculations,[21] we have studied the NQEs of H diffusion on the Pt(111) surface, and predicted the existence of atomic-scale resonance transmission phenomenon, i.e., atomic resonant tunneling (ART). For one-dimensional rectangular double barriers, the mathematical relation between the incident energy (E_i), the barrier height (E_b), and the energy and geometric parameters describing the double barriers has been established[22] for the resonant tunneling of quantum particles, in which 100% transmission takes place when $E_i < E_b$. Then, what about the transmission behavior of quantum particles (electrons, protons, ...) in the other types of potential fields? Additionally, a natural problem that follows is: For one-dimensional arbitrarily shaped double barriers of give heights, is it possible to realize the resonant tunneling of quantum particles when the barrier spacing can be tuned? In this work, based on the TM method, we have systematically investigated the NQEs of proton transfer in the fields of one-dimensional model potentials. The transport of protons across a series of model potential fields has been studied. The quantum probabilities of crossing rectangular, triangular, sine, parabolic single barriers, and single potential wells, and the corresponding double barriers are calculated. It is found that atomic resonant tunneling presents not only in the rectangular single potential wells and rectangular double barriers as expected, but also in the other shapes of potential wells and double barriers. In contrast, for hetero-structured double barriers, resonance transmission phenomenon, or ART is not seen in the classical forbidden zone when the incident energy is lower than the barrier height ($E_i < E_b$). Based on analytical calculations, we have analyzed the transmission coefficients of the hetero-structured double barriers in the rectangular case.

2. Results & discussion

2.1. Numerical calculations based on the TM method

We employ the transfer matrix method to calculate the quantum probabilities of protons transferring cross the model potentials. For a given potential filed $V(x)$, the incident and outgoing amplitudes (A_L, B_L; A_R, B_R) of the particle wave functions may be related by the transfer matrix $\boldsymbol{M}$ as follows:

$$\begin{pmatrix} A_R \\ B_R \end{pmatrix} = \boldsymbol{M} \begin{pmatrix} A_L \\ B_L \end{pmatrix} \equiv \begin{pmatrix} m_{11} & m_{12} \\ m_{21} & m_{22} \end{pmatrix} \begin{pmatrix} A_L \\ B_L \end{pmatrix}. \tag{1}$$

For the systems which preserve the time-reversal symmetry, the determinant $|\boldsymbol{M}| = 1$, and the transmission coefficient is given by $T_r(E) = 1/|m_{22}|^2$. More details of this method can be found in our recent work.[21]

We begin with investigating the transmission probability of individual H atoms passing through some model potentials of simple forms, as shown in Fig. 1. Four different types of single barriers (rectangle, triangle, parabola, and sine) with a width of 3 Å and a height of 0.5 eV are considered and compared. The single barrier width, 3 Å, is approximately the lattice spacing between the same type of adjoining surface sites (top-top, hcp-hcp, fcc-fcc) on Pt(111) surface.[21] As schematically shown in Fig. 1, the incident H atoms are from the left side of the barriers in the form of plane waves. The right panels of Fig. 1 display the transmission probabilities obtained from the TM method and the semi-classical method, the Wentzel–Kramers–Brillouin (WKB) approximation,[23] to make a comparison. For a given energy barrier $V(x)$, the latter computes the transmission probability as follows:

$$T_r(E) = \exp\left(-\frac{2}{\hbar}\int_a^b \sqrt{2m(V(x)-E)}\,\mathrm{d}x\right), \tag{2}$$

for $V(x) > E$ within the interval $a \le x \le b$, with m being the particle mass; and $T_r(E) = 1$ when $V(x) \le E$.

From Fig. 1, one sees that for all types of barriers the values of $T_r(E)$ increase sharply when the incident energy is close to the barrier height ($E_b = 0.5$ eV). Moreover, for the energy range of $E < E_b$, it can be seen that the transmission probabilities calculated by TM method (black lines) and WKB (red lines) are quantitatively comparable. The coincidence is further demonstrated by the corresponding logarithmic values of $T_r(E)$, as shown in the insets of the right panels of Fig. 1. The results indicate that in the range of $E < E_b$, WKB approximation can well predict the tunneling probability of particles across a single barrier. In contrast, when the incident

energy exceeds the barrier height (E_b), WKB fails to properly describe the transmission behavior, especially for the single rectangular barrier.

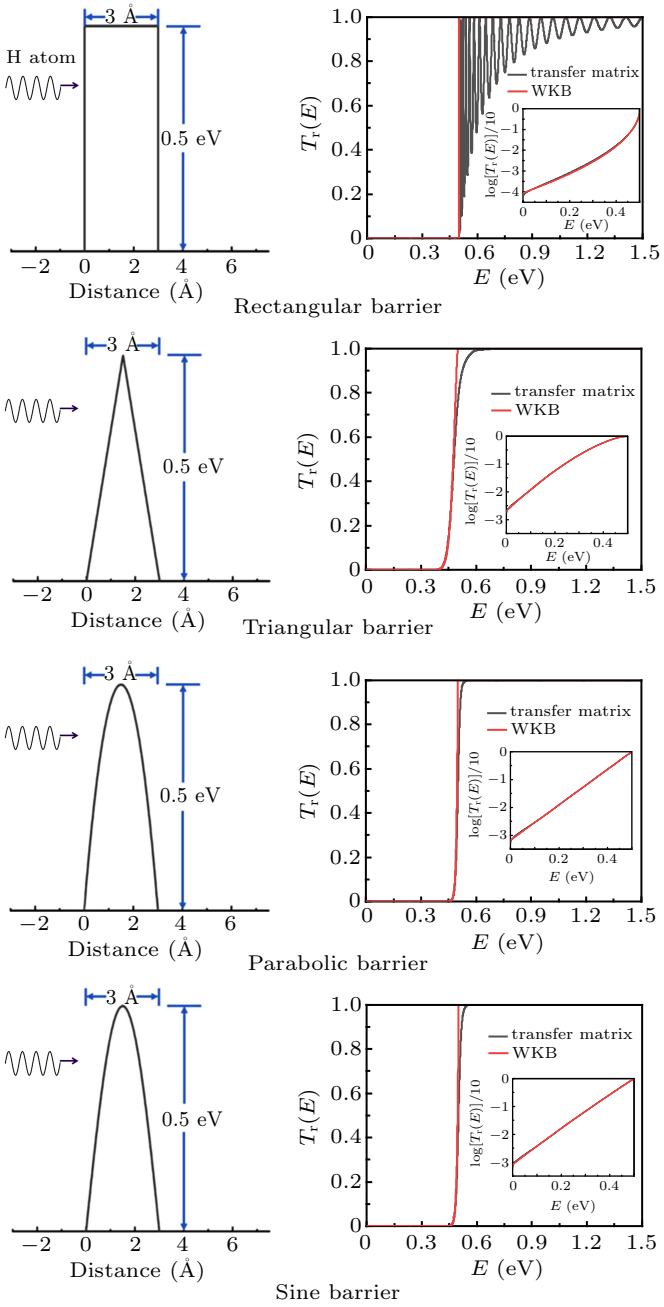


Fig. 1. Schematic diagram of H atoms crossing different types of single barriers (left panels), and the comparison of transmission probability calculated by the TM and WKB method (right panels), as a function of the incident energy E.

As shown in Fig. 1, when the incident energy is greater than 0.5 eV, the transmission probability calculated by TM method shows significant oscillation, while WKB can only give the result of complete transmission. This is another important feature that distinguishes quantum particles from classical ones. The reason why the quantum oscillations obtained by TM method are washed out in WKB approximation lies in the fact that the role of phase factors of particle wave functions which would induce quantum interference is explicitly included in TM method[21] while is absent in WKB. In addition, it can be found that the transmission behavior of the triangular, parabolic, and sine barriers with relatively similar barrier shapes is also similar. In particular, the transmission probabilities of the parabolic and sine barriers are almost the same. Compared with the rectangular single barrier, the potential fields change much more smoothly in the triangular, parabolic, and sine barriers; and the probabilities of barrier-crossing increase monotonically with the particle energy and finally approach 1. When the incident energies are higher than the barrier height, there is no quantum oscillation behavior as observed when crossing the rectangular barrier. This implies that the rate of change of the barrier in real space, $\mathrm{d}V/\mathrm{d}x$, may have nontrivial effects on the transmission behavior when passing through a given potential filed. For the situation where the potential changes drastically, such as the rectangular barrier, there will be significant quantum oscillations in the transmission probability. In the following, one can see that for single potential wells and double barriers, such a qualitative trend of variation still holds. Using the TM method, the transmission coefficient across a single rectangular barrier (barrier height: V_0; barrier width: a) may be expressed as follows:

$$T_r(E) = \left[1 + \frac{1}{\frac{E}{V_0}\left(1-\frac{E}{V_0}\right)}\mathrm{sh}^2(\beta a)\right]^{-1}, \tag{3}$$

where $\beta = \sqrt{2m(V_0-E)/\hbar^2}$. In the case of $E > V_0$, β is a complex number and Eq. (3) changes to

$$T_r(E) = \left[1 - \frac{1}{\frac{E}{V_0}\left(1-\frac{E}{V_0}\right)}\sin^2(\beta' a)\right]^{-1}, \tag{4}$$

where $\beta' = \sqrt{2m(E-V_0)/\hbar^2}$. The term $\sin^2(\beta' a)$ explains the long-range quantum oscillations of transferring across a single rectangular barrier (Fig. 1). In the case of $E \gg V_0$, $E/V_0 \gg 1$, to the first order of Taylor series, Eq. (4) may be further simplified to

$$T_r(E) \approx \left[1 + \left(\frac{V_0}{E}\right)^2 \sin^2(\beta' a)\right]^{-1} \approx 1 - \left(\frac{V_0}{E}\right)^2 \sin^2(\beta' a).$$

It is clear that the long-range oscillations originate from the second term which oscillates as a sine function of the incident energy, to large distances well above the barrier width.

We next study the transmission behavior of H atoms across a single potential well, which is geometrically the opposite of a potential barrier in real space. For a classical particle, the transmission probability is 1. For a quantum particle, the situation is much more different. Similar to the study of single barrier, four single potential wells of different shapes (rectangle, triangle, parabola, sine) with the width of 3 Å and the depth of 0.5 eV are considered. The right panels of Fig. 2 show the transmission probability calculated by the TM

method, with the incident energy ranging from 0 to 0.8 eV. For all types of potential wells, the most remarkable common feature is the phenomenon of resonant tunneling of H atoms, which shows $\sim 100\%$ transmission and takes place at discrete energy points.

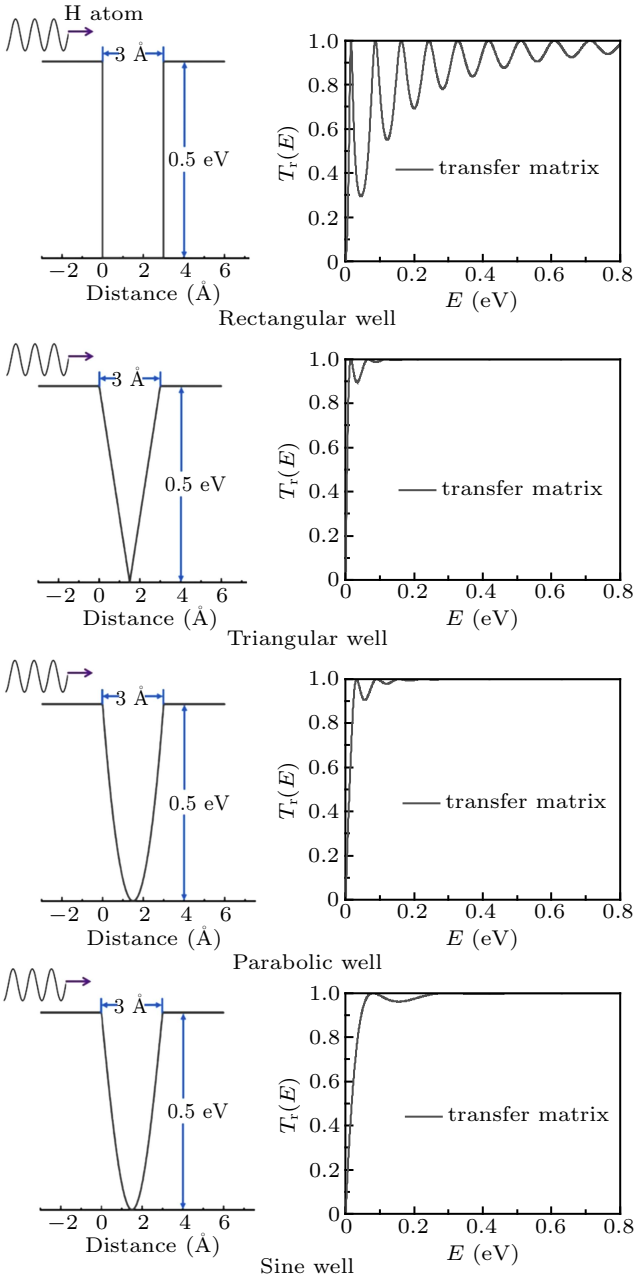


Fig. 2. Similar to Fig. 1 but for H passing through different types of single potential wells, which are studied using the TM method only.

Meanwhile, it can be seen that for the rectangular single potential well, there are significant oscillations for the incident energies well above the first energy point of resonant tunneling. For the other types of potential wells, however, after reaching the first peak of resonant tunneling, the variations of the tunneling probability are relatively flat and converge quickly to full transmission. This is similar to the situation of a single barrier, for which sharp changes present at boundaries of the potential field, and significant quantum oscillation occurs in the transmission probability; while transmission across the other three types of potentials wells shows much smaller magnitude of oscillations and converges quickly to 1.

The next model potentials we pay attention to are double barriers, which are the prototype of some important semiconducting devices. On both experimental and theoretical sides, extensive efforts have been devoted to the studies of resonance transmission of electrons across double barriers.[22,24–27] What about the much heavier H atoms/protons? As shown in Fig. 3, for different types of double barriers, resonant tunneling of H atoms can occur when appropriate physical conditions are chosen. Similar to the studies of single barriers and wells, four double barriers of different shapes (rectangle, triangle, parabola, sine) are considered: Each single barrier has a width $b = 1$ Å, a height of 0.2 eV, and a spacing $w = 1.4$ Å between each other. The right panels of Fig. 3 show the transmission probability calculated by the TM method for an energy interval of 0–0.4 eV. Intense peaks appear when the incident energy is close to the barrier height (0.2 eV), for all the double barriers with the tunneling probabilities close or equal to 1 (resonant tunneling). One can also see that, similar to the case of single barriers and single potential wells, for the rectangular double barriers with sharply varying potential fields at the boundaries, the energy range of the quantum oscillation of transmission probability is significantly larger than the other three situations when $E > E_b$. Further analysis shows that when the oscillation amplitude of the transmission probability converges to the level of $\sim 1\%$ (the corresponding energy point may be called the convergence radius), different types of barriers are quantitatively recognized using the convergence radius. For single barriers, the convergence radius of the rectangular, triangular, parabolic, and sinusoidal forms is 2.6460 eV, 0.5966 eV, 0.5326 eV, and 0.5374 eV, respectively. Their corresponding potential wells have a convergence radius of 2.2343 eV, 0.0969 eV, 0.1374 eV, and 0.2370 eV, respectively. Finally, the convergence radius of their corresponding double barriers is 1.4288 eV, 0.3528 eV, 0.3041 eV, and 0.2784 eV, respectively. In all cases it is clear that the potential fields consisting of rectangular barriers/wells show much larger convergence radii of quantum oscillation in the transmission probability than other types of model potentials. To show the role of inter-barrier spacing, we have also calculated the transmission coefficients for the double barriers configurations where the barrier-barrier spacing $w = 2$ Å. The results are displayed in Fig. 4. For the rectangular double barriers, a significant change is the disappearance of resonant tunneling at $E < E_b$ in the case of $w = 2$ Å. This is a demonstration of the role of phase factor difference which is related to the distance travelled by the particle.[22] Another notable change is the number of peaks appearing at $E < E_b$: For rectangle, triangle, parabola, and sine type double barriers, the number is

respectively 1, 3, 4, and 3 in Fig. 3 ($w = 1.4$ Å), while it is 1, 4, 3, and 5 in Fig. 4 ($w = 2$ Å), respectively.

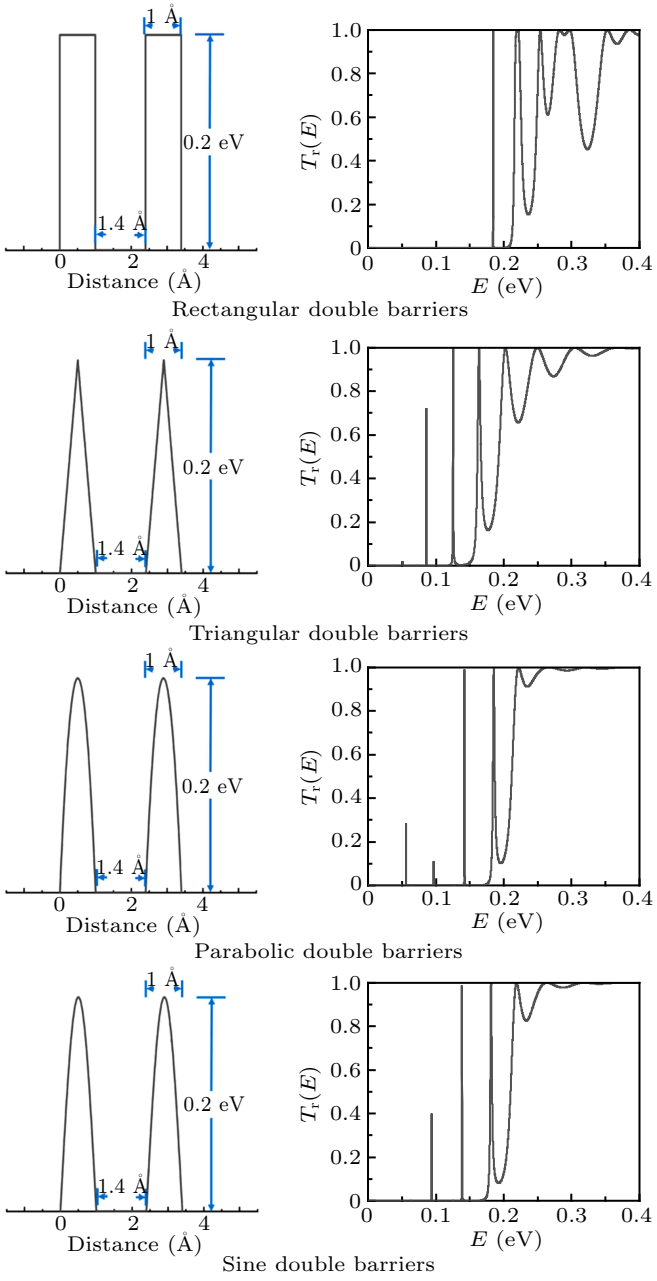


Fig. 3. Transmission properties of protons across homo-structured double barriers, calculated using the TM method.

The double barriers studied in Fig. 3 are homo-structured, i.e., the double barriers consist of the single barriers of identical geometric shapes. In the following, we go on to study the tunneling behavior of H atoms across hetero-structured double barriers, i.e., each of the component single barriers is different in geometry but with the same barrier height E_b. Figure 5 shows hetero-structured double barriers in which the pairs of single barriers have different types of geometric shapes but with the same barrier widths. From the top to bottom panels of Fig. 5, the combination of single barriers is rectangular–triangular, rectangular–parabolic, rectangular–sine, and triangular–sine, respectively. In all cases, the barrier–barrier spacing is 1.4 Å and the width of each single barrier is 1 Å with a barrier height of 0.2 eV. The corresponding transmission coefficients ($T_r(E)$) are plotted in the right panels, as a function of the incident energy of protons. To make a comparison, the hetero-structured double barriers in which the component single barriers belong to the same types of geometric shapes but with different barrier widths are also investigated, as schematically shown in Fig. 6. For each pair of single barriers constituting the double barriers, the barrier–barrier spacing is 1.4 Å, and the width is 1 Å for the narrower barrier and is 2 Å for the wider one. Like the ones studied in Fig. 5, the height of each single barrier is 0.2 eV. Similar to Fig. 5, the calculated transmission coefficients using the TM method are

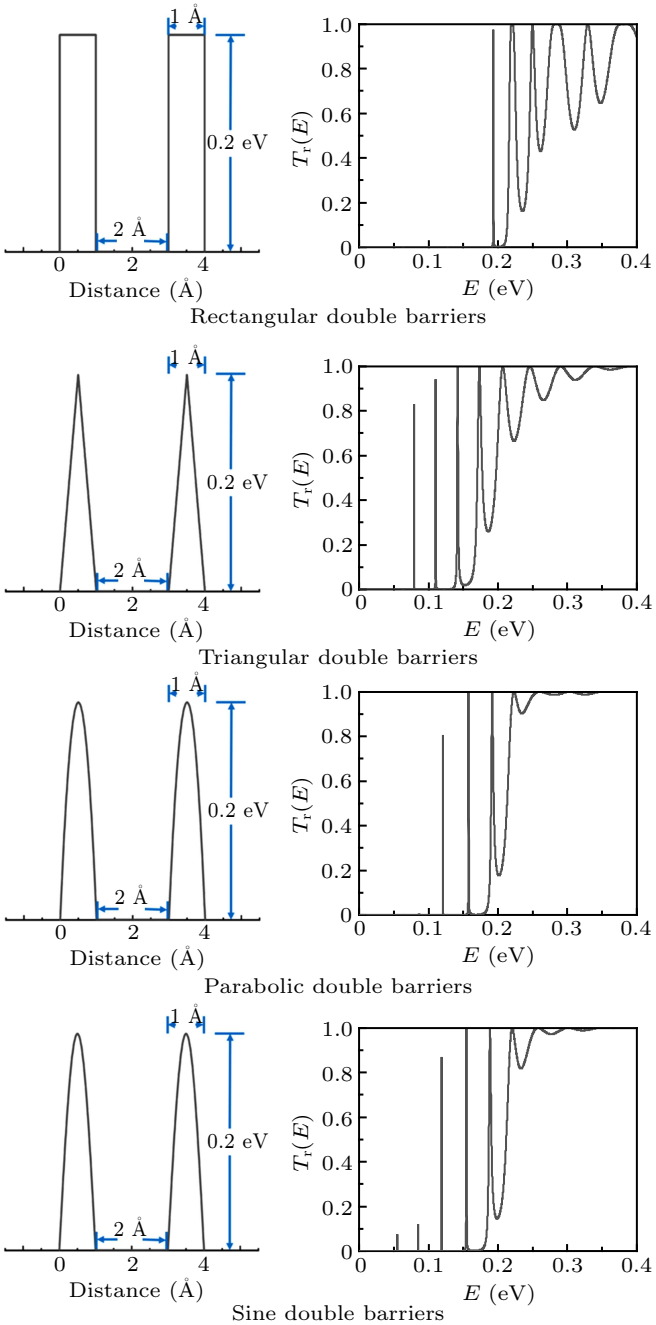


Fig. 4. Similar to Fig. 3 but for the situation where the inter-barrier spacing is 2 Å.

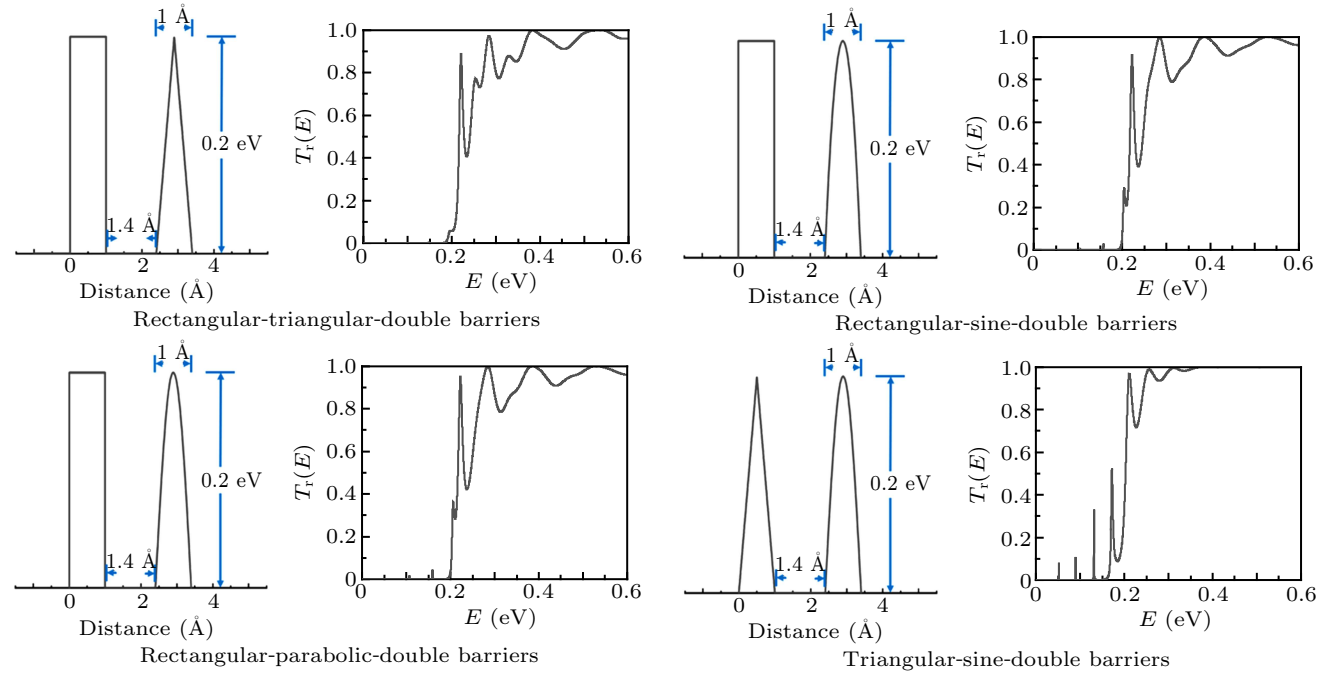


Fig. 5. Similar to Fig. 3 but for protons across hetero-structured double barriers which consist of single barriers of the same width but different types.

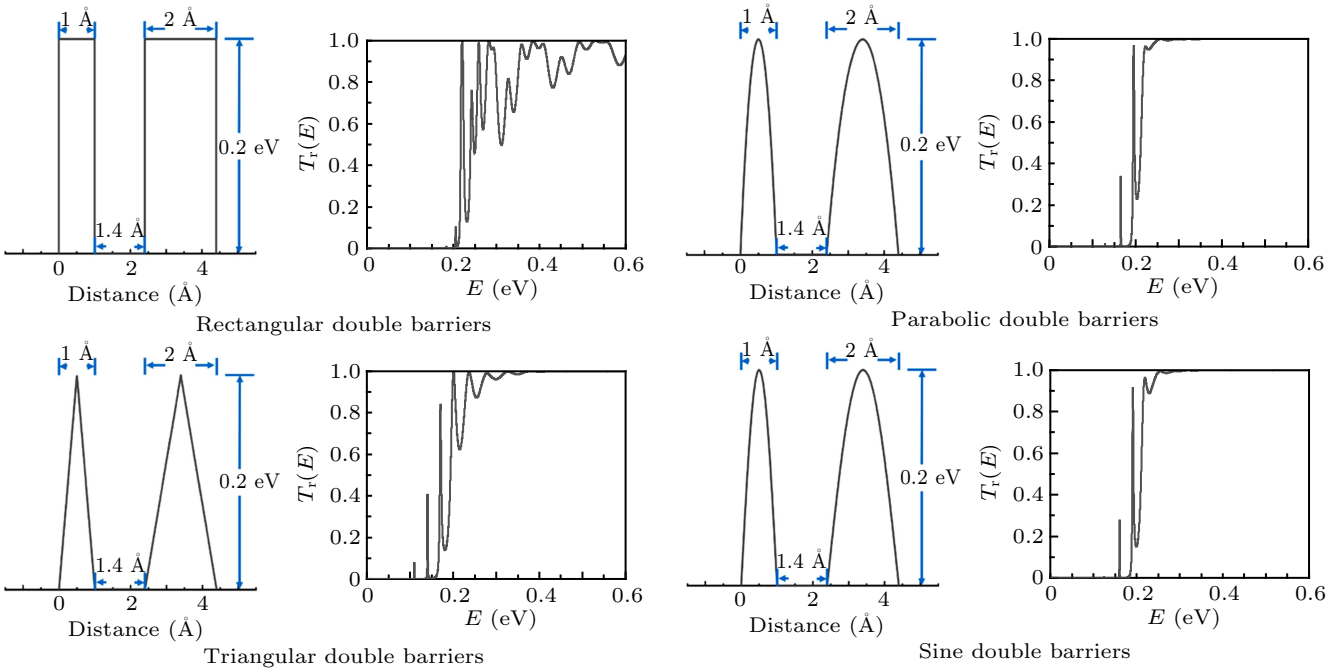


Fig. 6. Similar to Fig. 3 but for protons across hetero-structured double barriers which consist of single barriers of different widths but the same type.

displayed in the right panels of Fig. 6. From both Figs. 5 and 6, one can find that in all cases the transmission coefficients are always smaller than 1, i.e., $T_r(E) < 1$ when the incident energy is lower than the barrier height ($E_i < E_b$). This indicates the absence of atomic resonant tunneling (ART) when protons transfer across hetero-structured double barriers.

2.2. Theoretical analysis on hetero-structured rectangular double barriers

In this section, we perform theoretical analysis on the general transmission properties of quantum particles across hetero-structured double barriers, based on the analytic calculations using the TM method.

We firstly consider rectangular barriers. As illustrated in Fig. 7(a), for a single rectangular barrier, the wave functions on the left and right sides upon transmission across the barrier may be expressed in the following form:

$$\begin{cases} \psi_L(x) = A_L e^{iqx} + B_L e^{-iqx}, & (x < 0), \\ \psi_R(x) = A_R e^{iqx} + B_R e^{-iqx}, & (x > b), \end{cases} \tag{5}$$

where $q = (2mE/\hbar^2)^{1/2}$, with m being the particle mass, E the incident energy, and $\hbar$ the reduced Planck's con-

stant; and the parameters $A_{\rm L}$, $A_{\rm R}$, $B_{\rm L}$, and $B_{\rm R}$ are related by the transfer matrix $\boldsymbol{M}$ as shown in Eq. (1), which gives $\begin{cases} A_{\rm R} = m_{11}A_{\rm L} + m_{12}B_{\rm L} \\ B_{\rm R} = m_{21}A_{\rm L} + m_{22}B_{\rm L} \end{cases}$. When the single barrier is shifted along x-direction by a distance of $d = b + w$, as schematically shown in Fig. 7(b), the updated transfer matrix is[28]

$$\begin{aligned} \boldsymbol{M}(d) &= \begin{pmatrix} m_{11} & m_{12}\,\mathrm{e}^{-\mathrm{i}2qd} \\ m_{21}\,\mathrm{e}^{\mathrm{i}2qd} & m_{22} \end{pmatrix} \\ &= \begin{pmatrix} m_{11} & m_{12}\,\mathrm{e}^{-\mathrm{i}2q(b+w)} \\ m_{21}\,\mathrm{e}^{\mathrm{i}2q(b+w)} & m_{22} \end{pmatrix}. \end{aligned} \tag{6}$$

For double barriers which consist of single rectangular barriers with the same height (V_0) but different widths (a and b, respectively), and with a barrier-barrier spacing of w, the total transfer matrix is given by

$$\begin{aligned} \boldsymbol{M}_{\rm tot} &= \boldsymbol{M}(d)\,\boldsymbol{M}' \\ &= \begin{pmatrix} m_{11} & m_{12}\,\mathrm{e}^{-\mathrm{i}2q(b+w)} \\ m_{21}\,\mathrm{e}^{\mathrm{i}2q(b+w)} & m_{22} \end{pmatrix} \begin{pmatrix} m'_{11} & m'_{12} \\ m'_{21} & m'_{22} \end{pmatrix}, \end{aligned} \tag{7}$$

where the transfer matrix $\boldsymbol{M}'$ corresponds to the transmission process across the first rectangular barrier with a width of a, which differs from $\boldsymbol{M}$ mentioned above due to different width. The detailed form of $\boldsymbol{M}_{\rm tot}$ is

$$\boldsymbol{M}_{\rm tot} = \begin{pmatrix} m_{11}m'_{11} + m_{12}m'_{21}\,\mathrm{e}^{-\mathrm{i}2q(b+w)} & m_{11}m'_{12} + m_{12}m'_{22}\,\mathrm{e}^{-\mathrm{i}2q(b+w)} \\ m_{21}m'_{11}\,\mathrm{e}^{\mathrm{i}2q(b+w)} + m_{22}m'_{21} & m_{21}m'_{12}\,\mathrm{e}^{\mathrm{i}2q(b+w)} + m_{22}m'_{22} \end{pmatrix} \equiv \begin{pmatrix} M_{11} & M_{12} \\ M_{21} & M_{22} \end{pmatrix}. \tag{8}$$

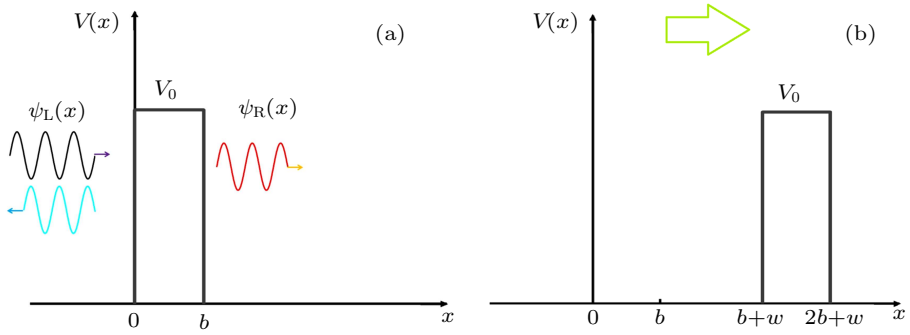


Fig. 7. (a) Schematics of scattering and transmission of a quantum particle by a potential barrier $V(x)$. (b) Translation of $V(x)$ by a distance.

The total transmission coefficient is given by

$$T_{\rm total} = 1/|M_{11}|^2. \tag{9}$$

Based on the results for single rectangular barriers,[21] each component of the matrix element M_{11} may be explicitly written as below:

$$\begin{aligned} m'_{11} &= \frac{\mathrm{e}^{-\mathrm{i}ka}}{4\mathrm{i}k\beta}\left[\mathrm{i}2k\beta + \left(\beta^2 - k^2\right)\right]\mathrm{e}^{\beta a} \\ &\quad + \left[\mathrm{i}2k\beta - \left(\beta^2 - k^2\right)\right]\mathrm{e}^{-\beta a}, \end{aligned} \tag{10a}$$

$$\begin{aligned} m_{11} &= \frac{\mathrm{e}^{-\mathrm{i}kb}}{4\mathrm{i}k\beta}\left[\mathrm{i}2k\beta + \left(\beta^2 - k^2\right)\right]\mathrm{e}^{\beta b} \\ &\quad + \left[\mathrm{i}2k\beta - \left(\beta^2 - k^2\right)\right]\mathrm{e}^{-\beta b}, \end{aligned} \tag{10b}$$

$$\begin{aligned} m_{12} &= \frac{\mathrm{e}^{-\mathrm{i}kb}}{4\mathrm{i}k\beta}\left\{\left(\beta^2 + k^2\right)\mathrm{e}^{\beta b} - \left(\beta^2 + k^2\right)\mathrm{e}^{-\beta b}\right\} \\ &= \frac{\mathrm{e}^{-\mathrm{i}kb}}{2\mathrm{i}k\beta}\left(\beta^2 + k^2\right)\sinh(\beta b), \end{aligned} \tag{10c}$$

$$\begin{aligned} m'_{21} &= -\frac{\mathrm{e}^{\mathrm{i}ka}}{4\mathrm{i}k\beta}\left\{\left(\beta^2 + k^2\right)\mathrm{e}^{\beta a} - \left(\beta^2 + k^2\right)\mathrm{e}^{-\beta a}\right\} \\ &= -\frac{\mathrm{e}^{\mathrm{i}ka}}{2\mathrm{i}k\beta}\left(\beta^2 + k^2\right)\sinh(\beta a), \end{aligned} \tag{10d}$$

where $k = \sqrt{2mE/\hbar^2}$, $\beta = \sqrt{2m(V_0 - E)/\hbar^2}$, and the width of the first and second rectangular barriers is a and b $(a \neq b)$, respectively. The square of modulus M_{11} is therefore given by

$$\begin{aligned} |M_{11}|^2 &= \left(m^*_{11}m'^*_{11} + m^*_{12}m'^*_{21}\,\mathrm{e}^{\mathrm{i}2q(b+w)}\right) \\ &\quad \times \left(m_{11}m'_{11} + m_{12}m'_{21}\,\mathrm{e}^{-\mathrm{i}2q(b+w)}\right), \\ &= |m_{11}|^2\left|m'_{11}\right|^2 + |m_{12}|^2\left|m'_{21}\right|^2 \\ &\quad + m_{11}m'_{11}m^*_{12}m'^*_{21}\,\mathrm{e}^{\mathrm{i}2q(b+w)} \\ &\quad + m^*_{11}m'^*_{11}m_{12}m'_{21}\,\mathrm{e}^{-\mathrm{i}2q(b+w)}. \end{aligned} \tag{11}$$

After substitution with the expressions presented in Eqs. (10a)–(10b), straightforward calculations give

$$\begin{aligned} |M_{11}|^2 &= 1 + \frac{\left(\beta^2 + k^2\right)^2}{4\beta^2k^2}\left[\sinh^2(\beta b) + \sinh^2(\beta a)\right] \\ &\quad + 2\left[\frac{\left(\beta^2 + k^2\right)^2}{4\beta^2k^2}\right]^2 \sinh^2(\beta b)\sinh^2(\beta a) \\ &\quad - \frac{1}{16k^4\beta^4}\left(\beta^2 + k^2\right)^2 \sinh(\beta b)\sinh(\beta a) \\ &\quad \times \left\{\left[\left(\beta^2 + k^2\right)^2 - 8k^2\beta^2\right]\cosh\beta(a+b)\right. \\ &\quad \left. - \left(\beta^2 + k^2\right)^2\cosh\beta(a-b)\right] \\ &\quad \times \cos 2\left[q(b+w) - ka\right] - 4k\beta\left(\beta^2 - k^2\right) \\ &\quad \times \sinh\beta(a+b)\sin 2\left[q(b+w) - ka\right]\Big\}. \end{aligned} \tag{12}$$

Consequently, the total transmission coefficient of a quantum particle passing across the hetero-structured rectangular double barriers is readily obtained using Eq. (9).

To further demonstrate the key difference that distinguishes hetero-structured double barriers from homo-structured double barriers, i.e., the existence or absence of resonant transmission, we have calculated the transmission coefficient of proton as a function of the ratio of the barrier width, b/a, for a given incident energy $E = 0.184$ eV, which gives ART for homo-structured rectangular double barriers shown in Fig. 3. During the calculations, the barrier height is kept at 0.2 eV with a barrier–barrier spacing of $w = 1.4$ Å, and the width of the first barrier is kept at $a = 1$ Å while the width of the second barrier varies from $b = 0.05$ Å to 10 Å. The results are shown in Fig. 8. Within the range of variation under consideration ($0.05 \leq b/a \leq 10$), it can be seen that if and only if $b/a = 1$, i.e., when the double barriers are homo-structured, the phenomenon of ART can happen.

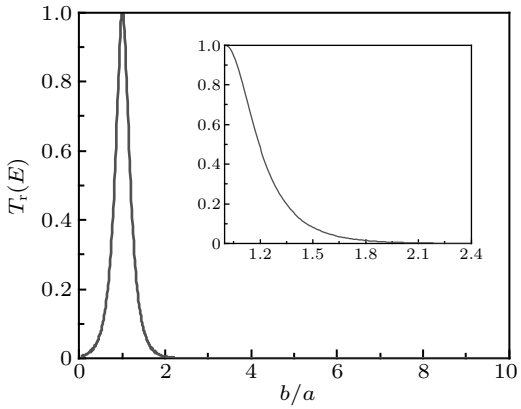


Fig. 8. Calculated transmission coefficients of protons transferring across hetero-structured rectangular double barriers, as a function of barrier width ratio.

3. Conclusions

We have studied the nuclear quantum effects (NQEs) on the processes of protons transferring across one-dimensional potentials fields (potential barriers and potential wells) by using the method of transfer matrix (TM), which is numerically accurate for the description of quantum particles transport in one-dimensional (1D) or quasi-1D systems. For the transfer of protons across single barriers, the transmission coefficients depend critically on the geometries of the barriers, where strong quantum oscillations are found in the case of rectangular barriers. The phenomenon of resonant transmission, i.e., atomic resonant tunneling (ART) of protons is demonstrated in various types of model potentials (single potential wells, homo-structured double barriers). By contrast, our calculations show that, ART is absent in hetero-structured double barriers which consist of single barriers of the same height but of different geometries. As an example of typical model potentials, rectangular hetero-structured double barriers are studied analytically and the mathematical expressions have been derived for the transmission coefficients of quantum particles in general. The absence of ART is again demonstrated by numerical calculations for rectangular hetero-structured double barriers.

References

[1] Howie R T, Scheler T, Guillaume C L and Gregoryanz E 2012 *Phys. Rev. B* **86** 214104
[2] Liu H and Ma Y 2013 *Phys. Rev. Lett.* **110** 025903
[3] Padalkar V S and Seki S 2016 *Chem. Soc. Rev.* **45** 169
[4] Liu S, Ma Y Z, Yang Y F, Liu S S, Li Y Q and Song Y Z 2018 *Chin. Phys. B* **27** 023103
[5] Yin H and Shi Y 2018 *Chin. Phys. B* **27** 058201
[6] Li H, Ma L, Yin H and Shi Y 2018 *Chin. Phys. B* **27** 098201
[7] Wang Y S, Jia M, Zhang Q L, Song X Y and Yang D P 2018 *Chin. Phys. B* **28** 103105
[8] Song Y, Liu S, Lu J, Zhang H, Zhang C and Du J 2019 *Chin. Phys. B* **28** 093102
[9] Horke D A, Watts H M, Smith A D, Jager E, Springate E, Alexander O, Cacho C, Chapman R T and Minns R S 2016 *Phys. Rev. Lett.* **117** 163002
[10] Liu P and Mei D 2020 *J. Phys. Chem. C.* **124** 22568
[11] Sofronov O O and Bakker H J 2020 *ACS Cent. Sci.* **6** 1150
[12] Andrade M F C, Ko H Y, Zhang L, Car R and Selloni A 2020 *Chem. Sci.* **11** 2335
[13] Markland T E and Ceriotti M 2018 *Nat. Rev. Chem.* **2** 0109
[14] Morales M A, McMahon J M, Pierleoni C and Ceperley D M 2013 *Phys. Rev. Lett.* **110** 065702
[15] McKenzie R H, Bekker C, Athokpam B and Ramesh S G 2014 *J. Chem. Phys.* **140** 174508
[16] Litman Y, Donadio D, Ceriotti M and Rossi M 2018 *J. Chem. Phys.* **148** 102320
[17] Andreani C, Colognesi D, Pietropaolo A and Senesi R 2011 *Chem. Phys. Lett.* **518** 1
[18] Senesi R, Flammini D, Kolesnikov A I, Murray É D, Galli G and Andreani C 2013 *J. Chem. Phys.* **139** 074504
[19] Guo J, Lü J T, Feng Y, Chen J, Peng J, Lin Z, Meng X, Wang Z, Li X, Wang E G and Jiang Y 2016 *Science* **352** 321
[20] Marx D and Parrinello M 1996 *J. Chem. Phys.* **104** 4077
[21] Bi C and Yang Y 2021 *J. Phys. Chem. C* **125** 464
[22] Hauge E H, Falck J P and Fjeldly T A 1987 *Phys. Rev. B* **36** 4203
[23] Schiff L I 1968 *Quantum Mechanics* (New York: McGraw-Hill) p. 268
[24] Tsu R and Esaki L 1973 *Appl. Phys. Lett.* **22** 562
[25] Chang L L, Esaki L and Tsu R 1974 *Appl. Phys. Lett.* **24** 593
[26] Choi K K, Levine B F, Malik R J, Walker J and Bethea C G 1987 *Phys. Rev. B* **35** 4172
[27] Zhang Y, Kastrup J, Klann R, Ploog K H and Grahn H T 1996 *Phys. Rev. Lett.* **77** 3001
[28] Grosso G and Parravicini G P 2014 *Solid State Physics* (Academic Press) p. 21